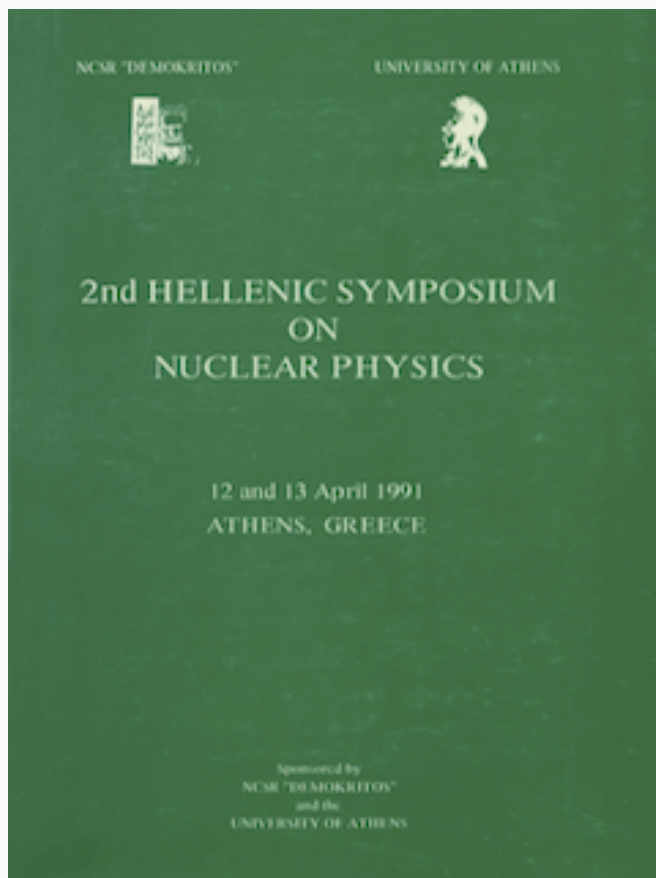


HNPS Advances in Nuclear Physics

Vol 2 (1991)

HNPS1991



FERMION-BOSON CLASSIFICATION IN MICROCLUSTERS

G. S. Anagnostatos

doi: [10.12681/hnps.2867](https://doi.org/10.12681/hnps.2867)

To cite this article:

Anagnostatos, G. S. (2020). FERMION-BOSON CLASSIFICATION IN MICROCLUSTERS. *HNPS Advances in Nuclear Physics*, 2, 407–426. <https://doi.org/10.12681/hnps.2867>

FERMION-BOSON CLASSIFICATION IN MICROCLUSTERS

G.S. ANAGNOSTATOS

Institute of Nuclear Physics

National Center for Scientific Research "Demokritos"

GR-153 10 Aghia Paraskevi Attiki, Greece

Abstract

Microclusters composed of atoms with *non* delocalized odd number of valence electrons possess the usual magic numbers for fermions in a central potential and those with an even number of valence electrons possess the magic numbers for bosons coming from the packing of atoms in nested icosahedral or octahedral or tetrahedral shells. On the other hand, microclusters composed of atoms *with* delocalized valence electrons, either with an odd or with an even number of electrons, exhibit electronic magic numbers (according to the jellium model) but *also* magic numbers coming from the (same, as above) packings of their bosonic ion cores. Finally, through the present work, an alternative approach to study atomic nuclei as quantum clusters appears possible and promising.

1. Introduction

Magic numbers (intensity anomalies in the mass spectra) in microclusters mainly have been interpreted as coming from two distinct and basically different origins which refer to separate categories of elements. That is, magic numbers are considered either as a result of electron structure (as in jellium model), e.g. in alkali clusters [1], or as a result of close packing of atoms, e.g. in rare gas clusters [2-3]. The magic numbers for these two categories are 2,8,20,40,58,... and 1,13,55,147,309,..... respectively. Recently however, it has been found that the magic numbers in certain mass spectra include numbers from both of the above sets [4-6]. Further complexity in understanding magic numbers comes from the fact that besides

those for alkali and rare gas clusters, different categories of magic numbers have been established for different elements or combinations of them. e.g., magic numbers for semiconductor [7] or alkali-halide clusters [8], or for clusters made of mixed rare gases [9] or mixed alkalis [10,11], etc.

The question raised by the present work is whether all these different sequences of magic numbers are indeed independent of each other or whether there is something fundamental, out of which one may derive them. In this paper, we propose a new concept that the magic numbers are mainly determined by the nature of particles involved in forming clusters. Depending on their odd or even number of electrons, the constituent atoms or ion cores behave as heavy fermions or heavy bosons. It is this property of constituent particles, together with the delocalized electrons, whenever they exist, that determine the structure of a microcluster [6].

2. The Model

2.1 Conceptualization of the model

The starting point of the present model is the comparative study of small-size-clusters of neutral and ionized alkali atoms shown in figures 1a, 1b, and 1c, which show, respectively, the celebrated experimental mass spectrum of sodium clusters [1], the prediction of the same in the jellium model, and the observed mass spectrum of sodium cluster cations [5].

The magic-number sequence in Figure 1(a) is 2,8,20,40,58,92,...., while the predicted magic numbers according to the jellium model (Figure 1(b)) are 2, 8, 18, 20, 34, 40, 58, 68, 70, 92,.... Thus, between the experimental data of Figure 1(a) and the jellium-model predictions there are differences. The model predicts additional peaks at $N= 18,34,68,70,....$ However, these missing numbers from Figure 1(a) are present in Figure 1(c), e.g., the peak at $N=19$ sodium cations which corresponds to 18 delocalized electrons ($N_e=N-1$) which is predicted by the jellium model. In addition, the spectrum in Figure 1(c) exhibits peaks at $N=13, (19), 25$ atoms, which are very well known as magic numbers of rare gas clusters [2-3]. Similar comments can be made when comparing other born neutral and born ionized small size alkali clusters.

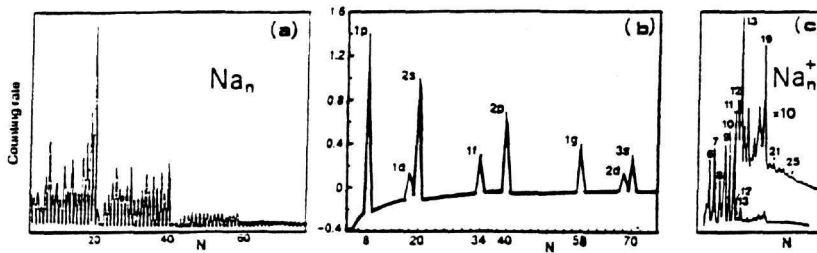


Figure 1(a)-(c). Mass spectra of sodium clusters. (a) Experimental data for neutral atoms, (b) jellium model predictions, and (c) experimental data for cations

One may therefore, infer that either a sodium mass spectrum does not include all predictions of jellium model (specifically the numbers 18,34,68,70,...) or it includes them but additional magic numbers, familiar from the close-packing of spheres structure (e.g., from the rare gas clusters), also exist. This is a general conclusion of all similar examples on alkali or alkali-like clusters.

The application of the jellium model implies that the valence electron from each alkali atom is delocalized and that all such electrons in the cluster move in a common central potential somehow created by the ion cores, a fact which leads to the electron magic numbers [1]. Indeed, there are experimental conditions which can secure the delocalization of the valence electrons, e.g., those valid for the experiment [5] of Figure 1(c). However, this is not necessarily the case in all experiments. Thus, if we do not have delocalization of valence electrons, one does not fulfill the assumption underlying the jellium model and electron magic numbers. Hence, Figure 1(a) can be seen as an example of localized electrons and thus the atoms themselves are the constituents of the cluster. In that case the jellium model is inapplicable. Also, the extra numbers (i.e., $N=13,19,25$) appearing in Figure 1(c) can be seen as magic numbers of the ion cores which are formed after the delocalization of valence electrons. Indeed, such ion cores do not exist when the constituents of the cluster are the neutral atoms themselves, a fact which is consistent with the absence of additional peaks in Figure 1(a).

2.2 Development of the Model

We present here a model where the nature of an atom or its ion core, taken as composite particles, is incorporated. That is, a neutral alkali atom (or a neutral atom of another element possessing an odd number of electrons) is considered as a heavy fermion due to its half integer total spin, while a neutral atom or an ion core possessing an even number of electrons is considered as a heavy boson due to its integer total spin [6].

Thus, in the model we are concerned not only with delocalized electrons and left-over ion cores, but also with atoms as particles. It is the Fermion or Boson nature of these particles rather than the forces among them that are emphasized in the model. The physical properties of Fermi- and Boson-like particles are different and they follow different statistics. Bosons usually occupy (if possible) the lowest available energy level, while Fermions occupy different energy levels, according to the Pauli principle.

In the model, each atom (or ion core) feels an average central potential created by all atoms (or ion cores) of a shell in the microcluster [6-12]. Inside this potential an atom (or ion core) moves independently from the motions of the other atoms (or ion cores). Of course, this model is analogous to that in nuclear physics. The difference is that the quantum constituent there is nucleons, whereas here it is the atoms (or ion cores) themselves which are either Fermions or Bosons, depending on their spin, determined by the number of electrons attached to them. This model should be distinguished from the jellium model [1], where the quantum constituent is the delocalized electrons and the central potential is somehow created by the ion cores. In this sense the jellium model is similar to the atomic shell model.

The model proposed herein is applicable, by itself, to a microcluster of neutral atoms. For the case of a microcluster composed of ionized atoms, the relevant model is a combination of the present model and the jellium model because the atomic-ion-cores are described by this model, whereas the electron motion is given by the jellium model. In this case the potential of the jellium model in general does not have, as usually assumed, an infinite spherical symmetry, but a reduced symmetry, determined by the structure of the ion cores. When the constituent atoms (either fermionic or bosonic) are neutral the magic numbers come from the structure of these atoms alone, and when the constituent atoms possess delocalized valence electrons, these numbers come from both the structure of the (always bosonic) ion cores and from the structure of the (fermionic) electrons [6].

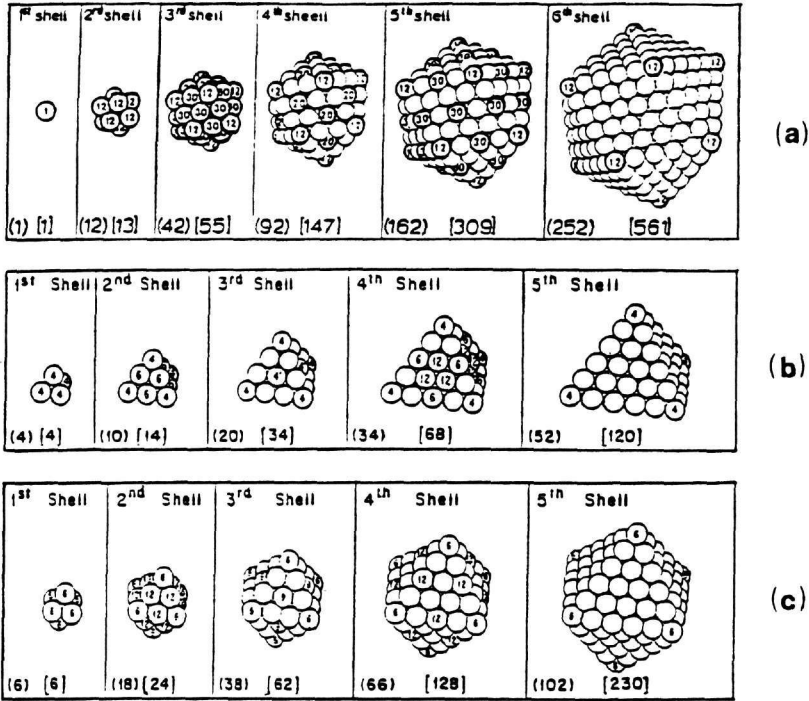


Figure 2(a)-(c). Close packing of *soft spheres* standing for atomic bosons (either as neutral atoms or as ion cores) in nested polyhedral shells. (a) icosahedra, (b) tetrahedra, and (c) octahedra.

In the model, the atoms are in continuous motion determined by their wave functions. However, the viscosity of the fluid formed by the atoms in the microclusters is much larger than that of the nucleons in the atomic nucleus, due to the much larger mass of the atoms compared to that of the nucleons. This large viscosity, of course, implies relatively slow motion of the atoms in the clusters. However, a geometrical structure of the cluster always results, if for each atom in the cluster one considers its average position. Such positions are discussed in [7-11,3,13-15] and are employed, e.g., in [6,12,15] in order to evaluate parameters of the relevant central potential needed for additional quantitative predictions by the present model. In refs [3,10,13], dealing

with fermionic clusters, the aforementioned average positions are simply useful *representations*, but in [3,7-9,14] dealing with bosonic clusters, these average positions form a structure which closely approximate the real structure of the relevant microcluster.

In Figure 2 the close packing of soft spheres standing for either neutral atoms or ion cores with an even number of electrons (bosons) is presented. In Figure 2(a) the first five successive shells of rare gas clusters are shown as nested icosahedral shells [3,9], while in Figure 2(b) and (c) those of semiconductor [7] and alkali-halide [8] clusters, as nested tetrahedral and nested octahedral shells, respectively, are presented. The relevant magic numbers are as follows: Figure 2(a) : $N=1, 13, 55, 147, 309, \dots$; Figure 2(b) : $N=4, 6, 10, 14, 18, 22, \dots$, also $5, 7, 11, 15, 19, 23, \dots$; Figure 2(c) : $N=6, 14, 18, 20, 24, \dots$, also $7, 10, 13, 17, 19, 25, \dots$ [3,7-8]

The initial choice for each specific cluster to assume one of the above three packing structures depends on the softness of spheres presenting the relevant atoms at each case. The softness of a sphere presenting an atom is a measure of the degree of completion of the outermost electronic shell of this atom and takes its minimum value (10%) when the outermost shells are complete, as in the case of rare gases [3], and larger values otherwise, e.g., for semiconductors (40%) and alkali-halides (30%).

The final choice among the three possibilities considered in Figure 2, dealing with bosonic constituent atoms (or ion cores), does not depend only on the softness of the relevant spheres mentioned above, but also on the temperature (or size) of the cluster. Indeed, a higher temperature or (very closely related) a larger size of a cluster corresponds to an excitation of the cluster which can alter the initial choice of structure and thus leads to a metastable structure. Thus, depending on the temperature and size of a cluster, a mixture of all magic numbers corresponding to all three parts of Figure 2 can be obtained in one and the same mass spectrum [6].

It is satisfying that shell structure based on nested tetrahedral, octahedral, and icosahedral packing simultaneously possesses stable equilibrium (which is necessary for the stability of a cluster) and minimization of electrostatic energy among atoms [16] of bosonic type occupying the lowest energy levels.

In Figure 3 the close packing of shells composed of hard spheres standing for neutral atoms with an odd number of electrons (fermions) is presented. In Figure 3(a) the first successive shells of alkali homoclusters are shown [3], while in Figure 3(b) and (c) those of alkali-heteroatoms [13] and of two kinds of alkali clusters [10] are shown. All three parts of Figure 3 are made up from nested equilibrium polyhedra as shown. It is satisfying that all

such polyhedra possess an equilibrium of the *average* positions of particles assumed on their vertices (middles of their edges or centers of faces) whatever the exact form of the force among fermion particles may be [16].

2.3 Simple Quantitative Treatment

The quantum mechanical treatment of rare gas microclusters (which here are representative clusters of bosonic atoms) has been presented in [17], based on a Path-Integral

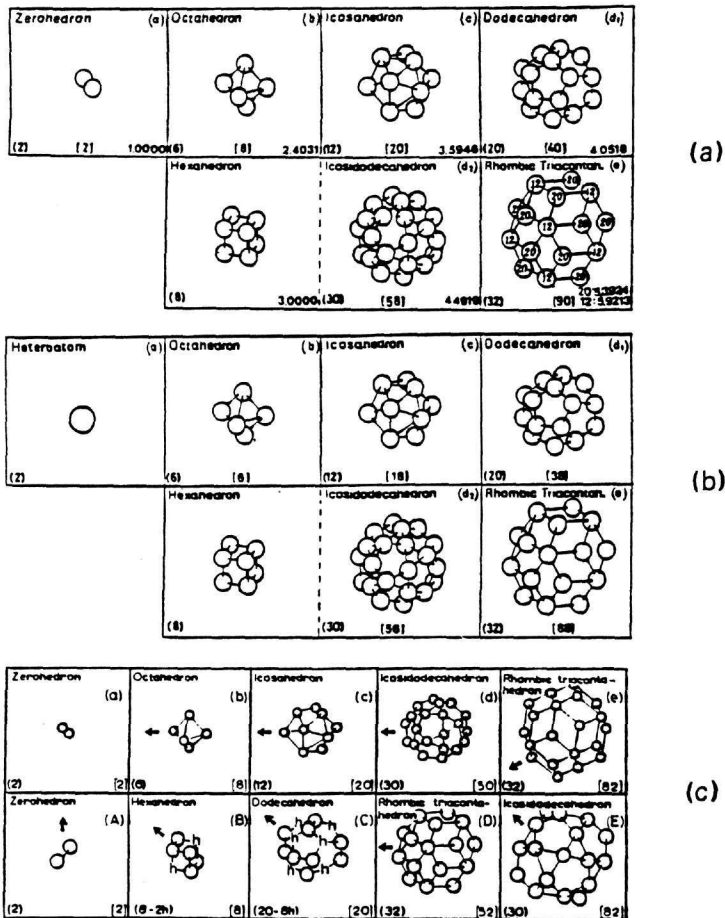


Figure 3(a-c). Close packing of shells composed of hard spheres standing for atomic fermions in nested equilibrium polyhedra. (a) Alkali homoclusters, (b) clusters of alkali heteroatom, and (c) two alkali clusters.

Monte-Carlo algorithm (instead of the wave function formalism), whereas treatment for alkali microclusters (which here are representative clusters of fermionic atoms) based on one body central forces has been studied in [12]. Here only some elements of a simple quantum mechanical treatment (taken from [12]), valid both for bosonic and fermionic atoms, are presented (and compared) taking advantage of the fact that both kinds of clusters form shells (called high fluximal shells) possessing a geometrical representation [3].

Here, the potential previously mentioned is better defined; it is specifically assumed that all atoms in a shell of the cluster taken together create an average central potential, assumed to be harmonic, common for all atoms in this shell and that in this potential each atom performs an independent particle motion obeying the Schrödinger's equation. In other words, we consider a multi-harmonic potential description of the cluster, as follows

$$H\psi = E\psi, \quad H = T + V \quad (2.3.1)$$

$$H = H_{1s} + H_{1p} + H_{1d2s} + \dots \quad (2.3.2)$$

where

$$H_i = V_i + T_i = -V + 1/2m(\omega_i)^2 r_i^2 + T_i \quad (2.3.3)$$

That is, we consider a state-dependent Hamiltonian, where each partial harmonic oscillator potential has its own state-dependent frequency ω_i . All these ω_i 's are determined from the harmonic oscillator relation (2.3.4)

$$h\omega_i = (h^2/m\langle r_i^2 \rangle) (n+3/2), \quad (2.3.4)$$

where n is the harmonic oscillator quantum number and $\langle r_i^2 \rangle^{1/2}$ is the average radius of the relevant maximal probability of occupation (hence forth called high fluximal) of a shell made of either bosonic [3,7-9,14] or fermionic [3,10,13] atoms. Before applying (2.3.4), to each of the shells a value (0,1,2,3,...) of the harmonic quantum number n is assigned and a value of $\langle r_i^2 \rangle^{1/2}$ is derived from the geometry of the shell taking the finite size of the atomic sphere into account. Thus, $h\omega_i$ changes value each time either n or $\langle r_i^2 \rangle^{1/2}$ (or both) changes its value.

In the case of bosonic atoms there is no restriction for the number of atoms in a shell, since any number of such atoms is accepted for the same quantum state (symmetric total wave function). In the case of fermionic atoms, however, the atoms on each shell are restricted by the Pauli principle (antisymmetric total wave function). It is satisfying that

all relevant shells for fermionic atoms [3,10,13] fulfil this fundamental requirement, as explained in detail in [12].

According to the Hamiltonian of (2.3.2), the binding energy, BE, of a cluster of N atoms is given by (2.3.5).

$$BE = 1/2 (VN) - 3/4 \left[\sum_{i=1}^N h\omega_i (n+3/2) \right], \quad (2.3.5)$$

where V is the average potential depth given [12] by (2.3.6)

$$V = -\alpha N + b + c/N, \quad (2.3.6)$$

The coefficient c in (2.3.6) expresses the sphericity of the cluster and has the same numerical value everywhere the outermost shell of the structure is completed and otherwise c has a zero value. Of course, one expects that different kinds of atoms will assume different values of parameters a, b, and c in (2.3.6).

The relative binding energy gap for a cluster with N atoms compared to clusters with N+1 and N-1 atoms is given by (2.3.7).

$$\delta(N) = 2E_B(N) - [E_B(N-1) + E_B(N+1)]. \quad (2.3.7)$$

As is apparent throughout the present work and the cited references, the average positions of the atoms (or their ion cores) in the clusters have a shell structure either for fermionic or for bosonic atoms. In this respect the structure of the clusters, to some extent, resembles nuclear structure.

Thus, several well-documented nuclear phenomena, e.g. collective effects, are reasonably expected for the clusters as well. Hence, small clusters of size N far from magic numbers are expected to be deformed. Furthermore, deformed (prolate or oblate) clusters are expected to rotate [18] and spherical (close to magic numbers) clusters are expected to vibrate. Besides these collective excitations, clusters can show single particle excitation either due to their atomic or electronic constituent (partial levels of ionization). All these interesting phenomena are out of the scope of the present work which mainly intends to obtain a classification of microclusters according to the statistics of the constituent atoms (i.e., Fermi or Boson statistics) depending on whether this constituent has half integer or integer spin.

3. Application of the Model

3.1 Alkali atoms without delocalized electrons

This category of clusters has been examined earlier [1] (See Sect. 2.1)

3.2 Alkali atoms with delocalized electrons

For example, in [4-5] dealing with Li_n^+ , Na_n^+ , and Rb_n^+ clusters, the appeared magic numbers are $N=3,5,7, 9,11,13, (15),19, 21, 23,(25),35,41,.....$ Out of these numbers, due to electron structure alone, magic numbers are predicted to be at $N=3,9,19,21,35,41$ (since for cations $N_e=N-1$). The remaining magic numbers, according to the present model, should come from the structure of the bosonic ion cores. Indeed, the numbers 13,19,(25) come from nested icosahedral packing [3] and the numbers 5,7,11,(15),19,23 from nested tetrahedral packing [7] with a central atom. In addition, it is satisfying that for negatively charged alkali clusters the magic numbers due to the ion cores remain the same [19].

3.3 Alkali-like atoms (Cu, Ag, Au)

These clusters are almost identical to alkali clusters. Because of the proximity of magic number 55 (due to ion cores) and of magic number 58 (due to electron structure), dramatic behavior is observed between 55 and 58 in all mass spectra of such atoms [19].

3.4 Even-valence atoms without delocalized electrons

In [20] for Pb_n the magic numbers are 10,13,15,17,19,23,25,..... It is satisfying that these numbers are almost identical to those discussed and explained previously for the ion cores of alkali clusters. Additional examples are in [21] and [22] for Co, Ni, and Ba.

3.5 Even-valence atoms with delocalized electrons

For born-ionized Zn_n^+ and Cd_n^+ [23] magic numbers appear at $N=10, 18, 20,28,30,$

32,35,41,46,54,57,60,69,.... Out of them the numbers $N=10, 18, 20, 30,35,46,57,69,...$ (with number of electrons 19,35,39,59,69,91,113,137,....) may be explained exactly or closed to the numbers predicted by the jellium model. With the exception of 41, all remaining magic numbers are interpreted by the nested octahedral [8] packing (e.g., the numbers 28,32, also 18,30) and by the nested tetrahedral [7] packing (e.g., the number 60).

3.6 Odd-valence atoms without delocalized electrons

In [24] for Nb clusters, the expected magic numbers for fermions 2 and 8 show up for light clusters, while for heavier clusters delocalization of electrons occurs (due to the higher temperature of the cluster) and the magic numbers 10,13,16,25,.... are exhibited [25]. With the exception of 16 all other numbers can be explained as close packing of ion cores [8].

3.7 Odd-valence atoms with delocalized electrons

Here, Al_n^+ is taken as an example [26]. Enhancements in mass spectra which appear at $N=3,7,14,20,23,...$ (with number of electrons 8,20,41,59,68,....) are explained by the jellium model, while enhancements at $N=5,10,15,18,...$ by the close packing of ion cores. Specifically, the first three are interpreted as nested tetrahedral shells [7], while the last one as nested octahedral shells [8].

3.8 Rare gas atoms

Since no valence electron exists here, all magic numbers come from the well known nested icosahedral shells [2,3].

3.9 Large size alkali clusters

In [27] large alkali clusters have been reported up to $N=22000$ atoms. According to this reference, the magic numbers for alkali clusters come, up to the size $N=1500$, from the electronic structure alone, while beyond this number, from shells of atoms alone. However, a closer examination of the experimental data of this reference, within the context of the present model, leads to different conclusions. Specifically, as shown in

Figure 4. shells of atoms exist even below $N=1500$ and electronic shells exist after this number as well [28].

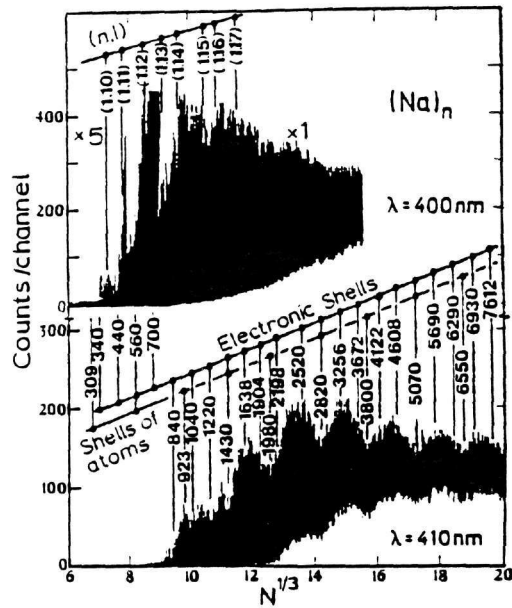


Figure 4. Coexistence of electronic shells and shells of atoms for sodium clusters. Positions marked by (n,l) values demonstrate the contribution of electronic subshells on the fine structure of the mass spectrum

The shells of atoms are estimated by using (3.9.1)

$$N_{\text{cluster}} = 1/3 (10K^3 - 15K^2 + 11K - 3) \quad (3.9.1)$$

(where K is a shell index) and the electronic shells (as groups of subshells having the same energy) by using the $3n+1$ approximate energy quantum number for alkali [27]. All these are supported by substantial minima in Figure 4. Even secondary minima all over the spectrum of Figure 4 (fine structure of the spectrum) are attributed to the electronic subshells, e.g., $(n,l)=(1,10), (1,11), (1,12), (1,13), (1,14), (1,15), (1,16), (1,17), \dots$

Thus, change of phase from the electronic shells to shells of atoms proposed in [27] is not supported by the present model. Such a change, however, is supported here

[12,29] in going from stochastic shells of atoms alone ($N < 70$) for born-neutral alkali clusters to the coexistence of electronic shells and shells of atoms ($N > 70$).

4. Extension of the Model to Nuclear Physics

The identity of light magic numbers in two independent branches of physics, alkali clusters and nuclear physics, obeying two basically different types of forces, electromagnetic and strong force, respectively, does not seem to be coincidental. This remark is in agreement with the fundamental premise of the present model, which emphasizes the statistical properties of the constituents (i.e., fermionic, bosonic nature) rather than the forces among them. The model clearly demonstrates that many properties can be understood directly from general consideration of the statistical properties rather than the strength of the particular force [10].

Many concepts and methods of treatment in cluster physics come from nuclear physics. However, the above remarks may be seen as a hint to reverse the flow of knowledge, now, from cluster physics to nuclear physics. The consideration of the size of nucleons via the sizes of their bags is essential, since we cannot speak about point nucleons in a structure resembling that of small clusters. We now apply specifically the model to nuclear structure employing 0.974 fm for the neutron bag and 0.860 fm for that of a proton [30]. These values are consistent with our knowledge from particle physics [31] that supports their relative size as well [32]. These different sizes of bags imply a weak isospin symmetry, or in other words they imply that a nucleus consists of two almost different (distinct) kinds of fermions. Thus, the nucleus resembles those of clusters which are made up of two kinds of alkalis [10], i.e., those presented by Figure 3(c).

The close packing of average sizes of shells assumed by this figure permits the determination of the average radial sizes of all nuclear shells with respect to the sizes of the nucleon bags alone. The necessary formula is [30]

$$R_x = \langle r^2 \rangle_{\text{shell}}^{1/2} = R \cos \alpha + (d^2 - R^2 \sin^2 \alpha)^{1/2}, \quad (4.1)$$

where R_x is the average radius of the shell to be determined, R the average radius of the previous shell in contact, d the distance of the centers of two nucleon bags in contact, and

α an angle defined by the symmetry and relative orientation of both shells involved each time in the calculation according to [33].

Now, the knowledge of the average radial size of all shells permits the determination of the average values of all nuclear radii (e.g., charge radii) by using (4.2), noted below, and assuming the filling of subshells according to the simple shell model [30].

$$\langle r^2 \rangle_{\text{nucleus}}^{1/2} = \left[\sum_1^Z \langle r^2 \rangle_i / Z + (0.8)^2 - (0.116)N/Z \right]^{1/2}, \quad (4.2)$$

where the $\langle r^2 \rangle_i^{1/2}$ values are given by (4.1) and the constants $(0.8)^2$ and (-0.116) are the ms charge radii accounting for the proton and the neutron finite sizes, respectively [34]. One can consult Table 1 for predictions of the model for all nuclei from H to Pb, where the only two parameters involved are the sizes of the neutron bag and the proton bag (specified above).

In Hamiltonian (2.3.3), besides the nuclear dimensions, we are concerned with the potential whose depth is taken from (4.3) and (4.4) noted below for neutron and protons, respectively [35].

$$-NV = -NV_0 + (27.2)(N-Z)/A, \quad (4.3)$$

and

$$-ZV = -ZV_0 - (27.2)(N-Z)/A + 2E_C/Z, \quad (4.4)$$

where the second term in each equation stands for the simplest possible isotope effect [36]. N, Z and A have their usual meaning, and E_C stands for the Coulomb energy [37], according to (4.5) below for $R=1.25 A^{1/3}$,

$$E_C = e^2/R [0.62Z(Z-1) - 0.46 Z^4/3], \quad (4.5)$$

and

$$NV_0 = ZV_0 = 79.26 - 0.0879 |A-74| \quad \text{for } A=16-74, \quad (4.6)$$

or

$$NV_0 = ZV_0 = 79.26 - 0.0313 |A-74| \quad \text{for } A=74-208, \quad (4.7)$$

The seven closed-shell nuclei in Table 2 are used for the determination of the three constants (parameters) in (4.6) and (4.7), while the nine open-shell nuclei of Table 3

Table 1. Charge root mean square radii in units Fermi

NUCL.	MOD.	EXP. ^a	NUCL.	MOD.	EXP. ^a
H		0.8	⁹⁸ Mo	4.40	4.391(26)
⁴ He	1.71	1.71(4)	⁹⁸ Tc	4.43	
⁷ Li	2.06	2.39(3)	¹⁰² Ru	4.46	4.480(22) ^d
⁹ Be	2.22	2.50(9)	¹⁰³ Rh	4.49	4.510(44)
¹¹ B	2.31	2.37	¹⁰⁶ Pd	4.52	4.541(33)
¹² C	2.37	2.40(56) ^b	¹⁰⁷ Ag	4.53	4.542(10) ^d
¹⁴ N	2.54	2.540(20)	¹¹⁴ Cd	4.57	4.624(8)
¹⁶ O	2.70	2.710(15) ^c	¹¹⁵ In	4.60	4.611(10) ^d
¹⁹ F	2.84	2.85(9) ^e	¹²⁰ Sn	4.63	4.630(7)
²⁰ Ne	2.98	3.00(3)	¹²¹ Sb	4.65	4.63(9)
²³ Na	2.95	2.94(4) ^e	¹³⁰ Te	4.67	4.721(6)
²⁴ Mg	3.06	3.08(5)	¹²⁷ I	4.72	4.737(7)
²⁷ Al	3.14	3.06(9)	¹³² Xe	4.77	4.790(22) ^d
²⁸ Si	3.21	3.15(5)	¹³⁵ Cs	4.82	4.801(11) ^d
³¹ P	3.27	3.24	¹³⁸ Ba	4.85	4.839(8) ^d
³² S	3.33	3.263(20)	¹³⁹ La	4.91	4.861(8)
³⁵ Cl	3.37	3.335(18)	¹⁴⁰ Ce	4.95	4.883(9)
⁴⁰ Ar	3.40	3.42(4)	¹⁴¹ Pr	4.99	4.881(9)
³⁹ K	3.44	3.436(3) ^e	¹⁴² Nd	5.03	4.993(35)
⁴⁰ Ca	3.47	3.482(25)	¹⁴⁶ Pm	5.06	
⁴⁵ Sc	3.51	3.550(5) ^e	¹⁵² Sm	5.10	5.095(30) ^d
⁴⁸ Ti	3.55	3.59(4)	¹⁵³ Eu	5.13	5.150(22) ^d
⁵¹ V	3.59	3.58(4)	¹⁵⁸ Gd	5.16	5.194(22) ^d
⁵² Cr	3.62	3.645(5) ^e	¹⁵⁹ Tb	5.19	
⁵⁵ Mn	3.65	3.68(11)	¹⁶⁴ Dy	5.22	5.222(30) ^d
⁵⁶ Fe	3.68	3.737(10)	¹⁶⁵ Ho	5.25	5.210(70) ^d
⁵⁹ Co	3.71	3.77(7)	¹⁶⁶ Er	5.23	5.243(30) ^d
⁵⁸ Ni	3.73	3.760(10)	¹⁶⁹ Tm	5.30	
⁶³ Cu	3.81	3.888(5) ^e	¹⁷⁴ Yb	5.32	5.312(60) ^d
⁶⁴ Zn	3.87	3.918(11)	¹⁷⁵ Lu	5.35	
⁶⁹ Ga	3.93		¹⁸⁰ Hf	5.37	5.339(22) ^d
⁷² Ge	3.99	4.050(32) ^d	¹⁸¹ Ta	5.40	5.500(200) ^d
⁷⁵ As	4.04	4.102(9) ^d	¹⁸⁴ W	5.42	5.42(7)
⁸⁰ Se	4.08		¹⁸⁷ Re	5.44	
⁷⁹ Br	4.13		¹⁹² Os	5.46	5.412(22) ^d
⁸⁶ Kr	4.17	4.160 ^e	¹⁹³ Ir	5.48	
⁸⁷ Rb	4.21	4.180 ^e	¹⁹⁵ Pt	5.50	5.366(22) ^d
⁸⁸ Sr	4.25	4.26(1)	¹⁹⁷ Au	5.52	5.434(2)
⁸⁹ Y	5.29	4.27(2)	²⁰² Hg	5.54	5.499(17) ^d
⁹⁰ Zr	4.32	4.28(2)	²⁰⁵ Tl	5.56	5.484(6)
⁹³ Nb	4.36	4.317(8) ^d	²⁰⁸ Pb	5.58	5.521(29)

^aThe experimental radii come from [34] except as noted below in b-d.

^b See [39]; ^c See [40]; ^d See [41].

constitute a sample of nuclei spread all over the table of isotopes for which the model makes real predictions. Specifically, nuclear charge radii come from (4.2) by using

Table 2: Binding energies and rms charge radii of closed-shell nuclei.

	¹⁶ O	⁴⁰ Ca	⁵⁸ Ni	⁹⁰ Zr	¹²⁰ Sn	¹⁴² Nd	²⁰⁸ Pb
E_C mod	12	65	123	223	331	447	757
EC emp	12	68	123	224	324	445	744
BE mod	125	350	495	782	1031	1185	1626
BE exp ^a	128	342	506	784	1021	1185	1637
$\langle r^2 \rangle^{1/2}$ mod	2.70	3.47	3.73	4.32	4.63	5.03	5.58
$\langle r^2 \rangle^{1/2}$ exp ^b	2.710	3.482	3.760	4.28	4.630	4.993	5.521
	(15)	(25)	(10)	(2)	(7)	(35)	(29)

^a See [42]; ^b See [34], [40], and [41]

Table 3: Predicted binding energies in MeV and rms charge radii in fm of a sample of ten open-shell nuclei close and far from magic numbers

	²⁸ Si	³⁶ Ar	⁴⁰ Ar	⁵⁶ Fe	¹⁰⁴ Pd	¹¹⁰ Pd	¹²⁶ Te	¹³⁶ Ba	¹³⁸ Ba	²⁰² Hg
E_C emp	30	50	55	107	280	280	345	392	390	713
BE mod	234	310	354	494	863	953	1067	1143	1157	1621
BE exp ^a	237	307	344	492	893	940	1066	1143	1159	1595
$\langle r^2 \rangle^{1/2}$ mod	3.21	3.41	3.40	3.68	4.52	4.51	4.67	4.86	4.85	5.54
$\langle r^2 \rangle^{1/2}$ exp	3.15 ^b	3.396 ^c	3.42 ^b	3.737 ^b	4.581 ^d	4.595 ^c	4.721 ^b	4.833 ^b	4.836 ^b	5.499 ^d
	(5)	(7)	(4)	(10)	(22)	(3)		(10)		(17)

^a See [42]; ^b See [34]; ^c See [40]; ^d See [41]

$\langle r^2 \rangle^{1/2}$ values from (4.1), while nuclear binding energies are calculated (2.3.5) by using h_{ij} values from (2.3.4) with the help of (4.1) and V values from (4.6 - 4.7).

All predictions of the model on radii and binding energies (see Tables 2 and 3) are satisfactory. This implies that an alternative method of studying atomic nuclei via quantum small-cluster concepts is possible and highly promising. Of course, a lot of work is necessary for the refinement of the method and its application to the whole spectrum of nuclear properties.

5. Concluding Remarks

The model introduced by the present paper, which is based on the nature of the constituent atoms or their ion cores, seems to be justified by all experimental data known to

us. Thus, the concept of fermionic and bosonic nature for atoms (or ion cores) with an odd and an even number of electrons respectively appears to combine the two views of electronic structure and atom-packing origin of magic numbers and at the same time to unify the comprehension of magic numbers in many kinds of clusters.

Specifically, clusters composed of atoms with non delocalized valence electrons and with an odd number of electrons have stochastic atom magic numbers alone at $N=2,8,20,40,\dots$ and those with an even number of electrons possess magic numbers coming from the packing of atoms alone in icosahedral or octahedral or tetrahedral form or mixed. On the other hand, clusters composed of atoms with delocalized valence electrons either with an odd or with an even number of valence electrons exhibit magic numbers due to the structure of their delocalized valence electrons but also magic numbers due to the packing of their (always bosonic) ion cores in forms similar to those discussed above.

Depending on the temperature or/and the size of the clusters, the forms (and thus the relevant magic numbers) of clusters assumed by bosonic atoms or bosonic ion cores (i.e., nested tetrahedra, or octahedra, or icosahedra) may change from the one (ground state) into the other form (excited or metastable structure). In a mixture of cluster sizes, i.e., in clusters with different temperatures, one may expect a coexistence of different forms and related magic numbers.

The state of matter of microclusters is apparently related to the present explanation. Specifically, bosonic clusters with no delocalized valence electrons are expected to closely resemble the solid state of matter (as it is known, e.g. for rare gas clusters), while fermionic clusters are expected to closely resemble the gas phase of matter (as it is believed, e.g. for alkali clusters) [38]. On the other hand, clusters with delocalized valence electrons (e.g. clusters born ionized), either bosonic or fermionic, are initially expected to have structure close to the solid state phase. However, due to the appearance of the ion cores in the cluster, a greater mobility of the constituent atoms exists, a fact which could shift the phase towards the structured liquids.

The equilibrium geometry of the average alkali shells in Figure 3 is not a fixed geometry like the one we are familiar with in solid state physics, but it simply is a geometrical representation of high fluxional shells like those we are familiar with from molecular orbitals.

Besides the novel quantum mechanical explanation of magic numbers, the present paper underlines the idea that *new*, as yet *unobserved* properties of microclusters should be investigated. Perhaps, the most important of them is the orbiting properties of atoms implying a series of properties due to orbital angular momentum, i.e., definite spin

properties, independent particle and collective modes of excitation of individual species, etc. For an experimental verification of such properties nuclear methods should be employed.

Finally, an alternative method of studying atomic nuclei via concepts of quantum clusters seems possible and promising. It seems that the clusters made up of two kinds of alkali atoms (two kinds of fermions) assume a structure close to nuclear (neutron and proton) structure. However, a lot of work towards this direction is still needed.

Acknowledgements

I express my sincere appreciation to Professors P. Jena, B.K. Rao and S.N. Khanna of the Virginia Commonwealth University, Department of Physics, for their support to the initial ideas of this work, and to Professors J.W. Negele and J. Goldstone of the M.I.T. Department of Physics for their invitations to join the highly stimulating scientific environment at their Center for Theoretical Physics in 1988-89 and 1990.

References

1. Ekardt, W: Phys. Rev. B **29**, 1558 (1984); Knight, W.D., Clemenger, K., de Heer, W.A., Saunders, W.A., Chow, M.Y., Cohen, M.L.: Phys. Rev. Lett. **52**, 2141 (1984).
2. Echt, O., Sattler, K., Recknagel, E.: Phys. Rev. Lett. **47**, 1121(1981).
3. Anagnostatos, G.S.: Phys. Lett. A **124**, 85(1987)
4. Saito, Y., Watanabe, M., Hagiwara, T., Nishigati, S., Noda, T.: Jpn J. Appl. Phys. **27**, 424(1988); Saito, Y., Minami, K., Ishida, T., Noda, T.: Z.Phys. D-Atoms, Molecules and Clusters **11**, 87(1989).
5. Bhaskar, N.D., Frueholz, R.P., Klimcak, C.M., Cook, R.A.: Phys. Rev. B **36**, 4418(1987).
6. Anagnostatos, G.S.: Phys. Lett. A **157**, 65 (1991).
7. Anagnostatos, G.S.: Phys. Lett. A **143**, 332(1990)
8. Anagnostatos, G.S.: Phys. Lett. A **150**, 303(1990)
9. Anagnostatos, G.S.: Phys. Lett. A **133**, 419(1988)
10. Anagnostatos, G.S.: Phys. Lett. A **128**, 266(1988)
11. Anagnostatos, G.S.: Z. Phys D - Atoms, Molecules and Clusters **19**, 121 (1991).

12. Anagnostatos, G.S.: Phys. Lett. A **154**, 169 (1991).
13. Anagnostatos, G.S.: Phys. Lett. A **142**, 146(1989).
14. Anagnostatos, G.S.: Phys. Lett. A **148**, 291(1990).
15. Anagnostatos, G.S.: Z. Phys. D-Atoms, Molecules and Clusters **19**, 125 (1991).
16. Leech, J.: Math. Gazette **41**, 81(1957).
17. Franke, G., Hilf, E., Palley, L.: Z. Phys. D-Atoms, Molecules and Clusters **9**, 343(1988).
18. Lipparini, E., Stringari, S.: Phys. Rev. Lett. **63**, 570(1989).
19. Katakuse, I., Ichihara, T., Fujita, Y., Matsuo, T., Sakurai, T., Matsuda, H.: Int. J. Mass Spectr. Ion Proc. **74**, 33(1986).
20. Mühlbach, J., Pfau, P., Sattler, K., Recknagel, E.: Z. Phys. B **47**, 233(1982).
21. Klots, T.D., Winter, B.J., Parks, E.K., Riley, S.J.: J.Chem. Phys. **92**, 2110(1990).
22. Rayane, D., Melnon, P., Cabaud, B., Hoareau, A., Tribollet, B., Broyer, M.: Phys. Rev. D-Atoms, Molecules and Clusters **39**, 6056(1989).
23. Katakuse, I., Ichihara, T., Fujita, Y., Matsuo, T., Sakurai, T., Matsuda, H.: Int. J. Mass Spectr. Ion Proc. **69**, 109(1986).
24. Geusic, M.E., Morse, M.D., Smalley, R.E.: J. Chem. Phys. **82**, 590(1985).
25. Whelton, R.L., Zakin, M.R., Cox, D.M., Trevor, D.J., Kaldor, A.: J. Chem. Phys. **85**, No.3(1986).
26. Begemann, W., Driehöfer, S., Meiwes-Broer, K.H., Lutz, H.O.: Z. Phys. D-Atoms, Molecules and Clusters **3**, 183(1986).
27. Martin, T.P., Bergmann, T., Göhlich, H., Large, T.: Chem. Phys. Lett. **172**, 209(1990).
28. Anagnostatos, G.S.: To appear.
29. Bjornholm, S., Borggreen, J., Echt, O., Hansen, K., Pedersen, J., Rasmussen, H.D.: Phys. Rev. Lett. **65**, 1627(1990).
30. Anagnostatos, G.S.: Int. J. Theor. Phys. **24**, 579(1985).
31. Thomas, A.W.: Adv. Nucl. Phys. **13**, 1(1984).
32. Celenza, L.S., Shakin, C.M.: Phys. Rev. C **27**, 1561(1983).
33. Coxeter, H.S.M.: Regular polytopes, 3rd Ed. (Macmillan, New York, 1973).
34. de Jager, C.W., de Vries, H., de Vries, C.: At. Data Nucl. Data Tables **14**, 479(1974).
35. Anagnostatos, G.S.: To appear.
36. Hornyak, W.F.: *Nuclear Structure*, Academic, New York, 1975.
37. Hill, D.L.: In *Encyclopedia of Physics*, Flugge, S. ed., Springer-Verlag, Berlin, vol. XXXIX, p. 211 (1957).
38. Gspann, G.: Z. Phys. D-Atoms, Molecules and Clusters **3**, 143(1986).

39. Engfer, R., Schneuwly, H., Vuilleumier, J.L., Valter, H.K., Zehnder, A.: *Atomic Data and Nuclear Data Tables* **14**, 509 (1974).
40. Brown, B.A., Bronk, C.R., Hodgson, P.E.: *J. Phys. G* **10**, 1683 (1984).
41. Wesolowski, E.: *J. Phys. G* **10**, 321 (1984).
42. Wapstra, A.H., Gove, N.B.: *Nuclear Data Tables* **9**, 267 (1971).